AGU ADVANCING EARTH AND SPACE SCIENCES

Geophysical Research Letters

RESEARCH LETTER
10.1029/2026GL121645

On the Biases of Empirical Riverine Gas Transfer Velocity Models at High Submergence

G. Dolcetti[1], **M. Brocchini**[2], **and A. Siviglia**[1]

[1]Department of Civil, Environmental and Mechanical Engineering, University of Trento, Trento, Italy, [2]Construction, Civil Engineering and Architecture Department, Marche Polytechnic University, Ancona, Italy

Key Points:

- Most data that were used to calibrate widely used empirical models for the gas transfer velocity are from low-submergence rivers
- Global carbon budget estimates based on these models may overestimate riverine CO_2 emissions by up to 24%
- We propose a method to reconstruct the unknown submergence information and correct gas exchange flux estimations at a global scale

Supporting Information:

Supporting Information may be found in the online version of this article.

Correspondence to:

G. Dolcetti,
giulio.dolcetti@unitn.it

Citation:

Dolcetti, G., Brocchini, M., & Siviglia, A. (2026). On the biases of empirical riverine gas transfer velocity models at high submergence. *Geophysical Research Letters*, *53*, e2026GL121645. https://doi.org/10.1029/2026GL121645

Received 3 JAN 2026
Accepted 9 APR 2026

Author Contributions:

Conceptualization: G. Dolcetti
Formal analysis: G. Dolcetti, M. Brocchini, A. Siviglia
Funding acquisition: A. Siviglia
Investigation: G. Dolcetti, M. Brocchini, A. Siviglia
Methodology: G. Dolcetti
Project administration: A. Siviglia
Visualization: G. Dolcetti
Writing – original draft: G. Dolcetti
Writing – review & editing: M. Brocchini, A. Siviglia

Abstract Quantifying gas transfer velocity in rivers, a key step in characterizing riverine ecosystems, carbon cycling, and greenhouse gas emissions, typically relies on empirical or semi-empirical models. Although fluid mechanics theory predicts a direct influence of the depth-to-bed-roughness-size ratio (relative submergence) on gas transfer velocity, the submergence is rarely reported in gas exchange data sets, and empirical models do not include it as an explanatory parameter. We derived a new approach based on hydraulic resistance equations to reconstruct the missing submergence information and correct gas transfer velocity models using common geometric and hydraulic quantities. We demonstrate a low-submergence bias in the calibration data of widely used empirical gas transfer velocity models, which explains their behavior and large disagreement at high submergence. We estimated the corrected carbon dioxide gas exchange fluxes for global rivers, and found that emissions from large, high-submergence (typically lowland) rivers are significantly lower and more uncertain than previously estimated.

Plain Language Summary Calculating the amount of gas exchanged between rivers and the atmosphere is a key step to measure and understand how rivers contribute to the carbon cycle, and how their role may change due to the climate crisis. Currently, the same models are used to calculate gas exchange in deep and shallow rivers, although the process that controls the gas exchange is very different if the flow depth is large or small compared to the size of the elements (e.g., sand, gravel, rock, etc.) that constitute the riverbed. We derived a method to estimate the size of bed elements, and found that existing models are not suitable for large rivers, since they were derived based on data from small rivers and streams. We corrected the models and recalculated the amount of carbon dioxide emitted globally by rivers. We found that emissions are significantly lower and more uncertain than previously estimated, especially in the largest rivers of the world.

1. Introduction

Gas exchange between rivers and the atmosphere is a key regulator of riverine ecology and biodiversity, and a fundamental pathway for carbon biogeochemistry (Dean & Battin, 2024). Rivers are increasingly recognized as strong emitters of greenhouse gases such as carbon dioxide, methane, and nitrous oxide toward the atmosphere (Lauerwald et al., 2023). The gas transfer velocity, k (m/s), is a key parameter representing the efficiency of the exchange process dominated by turbulent mixing near the water surface. Accurate estimations of k are critical for the correct calculation of gas exchange fluxes and the closure of the riverine carbon and oxygen balance, a fundamental step in quantifying ecosystem metabolism (Battin et al., 2023; Diamond & Bertuzzo, 2025). Due to the intrinsically local and small-scale nature of turbulent processes, direct measurements of the gas transfer velocity are challenging and fail to account for the highly dynamic and/or heterogeneous flow conditions of many rivers and streams (Hall & Ulseth, 2020).

Predicting k based on models is far more efficient and is currently the only practical way to calculate gas exchange fluxes at large scales. From a theoretical perspective, there is good consensus that gas exchange is controlled by small turbulent eddies that transport water parcels between the bulk of the flow and a very thin ($\sim$10 μm) sub-surface concentration boundary layer, where molecular diffusion drives the actual exchange (the so-called renewal model: Danckwerts, 1951; Lamont & Scott, 1970). As a result, k is a function of the Schmidt number ($\mathrm{Sc} = \nu/\mathcal{D}_m$, where ν and $\mathcal{D}_m$ are the molecular viscosity and diffusivity, respectively) and of the near-surface turbulent kinetic energy dissipation rate, ε, which governs the frequency of renewal by small eddies. To enable calculating ε as a function of more easily measurable bulk flow parameters such as the channel slope (S), water depth (H), and mean flow velocity (V), turbulence production can be assumed to be dominated by either bed

friction, or form drag, depending on the ratio between water depth, H, and bed roughness height, D (the so-called relative submergence, H/D). This results in two distinct expressions for ε in smooth or small-roughness flows (ε_s, Moog & Jirka, 1999a) and in macro-roughness-dominated flows (ε_d, Moog & Jirka, 1999b).

Theoretical expressions based on the small- or macro-roughness scaling of ε are used very seldom, possibly because of the difficulty in identifying the dominant driver of turbulence uniquely. Instead, k is usually calculated using empirical or semi-empirical functions of bulk flow parameters, calibrated on large field data sets. Two empirical models, in particular (Raymond et al., 2012; Ulseth et al., 2019), are most widely used and ordinarily employed to compute riverine gas fluxes from reach scale to global scale (e.g., Lauerwald et al., 2015; Liu et al., 2022). These models do not distinguish between small-roughness and macro-roughness-driven renewal, but they broadly agree with the macro-roughness formulation (Moog & Jirka, 1999b), even though they are commonly applied to both low- and high-submergence river conditions.

To better understand what drives the scaling of ε and of k and how scaling assumptions affect the estimation of riverine gas fluxes on a global scale, here we investigate the range of validity of the most widely used gas transfer velocity models (Raymond et al., 2012; Ulseth et al., 2019). We assume H/D to be the main driver of the transition between friction-dominated (high H/D) and form-drag-dominated (low H/D) turbulent mixing, affecting the dependence of k from bulk flow parameters (Moog & Jirka, 1999a, 1999b). Then, our goals are to reconstruct the range of submergence in the data sets that were used for calibrating the models of Raymond et al. (2012) and Ulseth et al. (2019), clarify if it is representative of the range expected in the applications, and calculate revised global riverine CO_2 emissions accounting for the broad range of submergence in global river systems.

2. Background

2.1. Relative Submergence Effects on Gas Transfer Velocity Scaling

The mass exchange flux F of a sparingly soluble gas across the air-water interface is generally described as $F = k(C - C_{eq})$, where C (mol/m^3) is the gas concentration in water and C_{eq} (mol/m^3) is the temperature-dependent atmospheric equilibrium concentration. While the dissolved gas concentration is the result of a variety of biogeochemical processes, k expresses mostly the physical drivers, namely the efficiency of turbulent mixing underneath the surface. According to the surface renewal model (Danckwerts, 1951) the gas transfer velocity can be calculated as $k = \sqrt{D_m/\tau_\eta}$, where τ_η is the eddy renewal period, which is well-represented by the Kolmogorov time scale. Under these assumptions, the surface renewal model predicts a power-function dependence of k on ε (Lamont & Scott, 1970)

$$k \sim \mathrm{Sc}^{-1/2}(\nu\varepsilon)^{1/4}. \tag{1}$$

To isolate diffusivity effects, k is often converted to a reference $\mathrm{Sc} = 600$ and expressed as k_{600}. The validity of Equation 1 is supported by laboratory and field experiments, and has been termed a "universal scaling" since it arises consistently from different analytical approaches, such as a structure-function-based interpretation (Katul & Liu, 2017) or dimensional analysis (Lorke & Peeters, 2006).

Bed friction (used here in place of the more restrictive term *skin friction*) characterizes flow conditions in which the near-bed and near-surface regions remain dynamically separated, such that the roughness-induced wake does not reach the surface (Moog & Jirka, 1999b). Under these conditions, the turbulence dissipation decreases exponentially with the distance from the bed and has the value of $\varepsilon = u_*^3/(2H)$ at the surface (Nezu & Nakagawa, 1993) (see Figure 1), where $u_* = \sqrt{gR_hS}$ is the shear velocity and R_h is the hydraulic radius. Hereafter, we consider $R_h \approx H$ assuming a large channel aspect ratio, without loss of generality. Moog and Jirka (1999a) used a different formulation without the factor 2 at the denominator, as follows:

$$\varepsilon_s = u_*^3/H. \tag{2}$$

The subscript s indicates that Equation 2 applies in smooth or high submergence flows ($H/D \gg 1$), where bed friction is the dominant turbulence production mechanism.

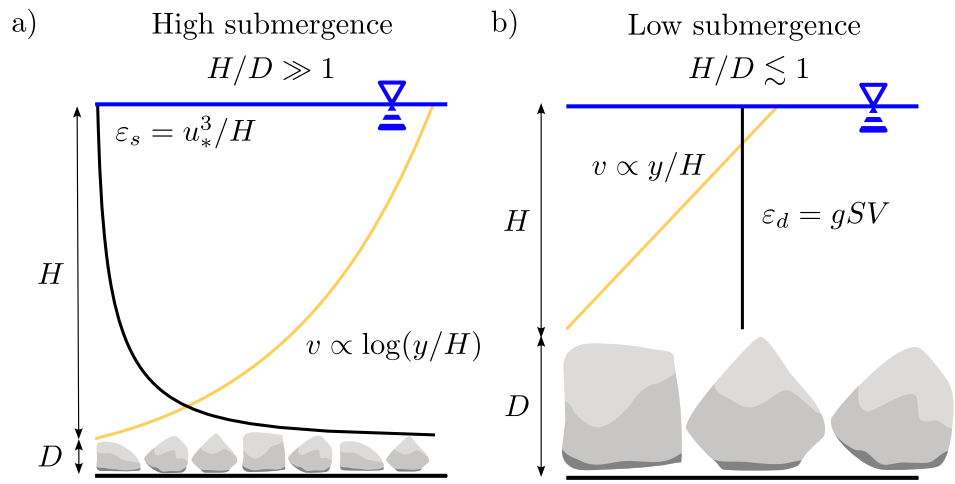

Figure 1. Distribution of (yellow) velocity and (black) turbulent kinetic energy dissipation rate, for (a) large-submergence flows (Moog & Jirka, 1999a), and (b) small-submergence flows (Moog & Jirka, 1999b).

On the contrary, in low submergence flows ($H/D \lesssim 1$), form drag and wake separation behind roughness elements (macro-roughness) contribute to the turbulence budget also near the surface. In such form-drag-dominated conditions, turbulence dissipation can be assumed to be everywhere equal to the total stream power, leading to (Moog & Jirka, 1999b)

$$\varepsilon_d = gSV, \tag{3}$$

where the subscript d indicates the dominant effect of drag.

Mixing in small-submergence conditions is generally more efficient. Therefore, the ratio between the small-submergence and high-submergence dissipation rates, $\varepsilon_d/\varepsilon_s = V/u_*$, is often large. In intermediate submergence conditions, Moog and Jirka (1999b) proposed calculating the turbulence dissipation rate as

$$\varepsilon_\phi = \phi\varepsilon_d + (1-\phi)\varepsilon_s \tag{4}$$

where the subscript ϕ indicates the dependence on an unknown coefficient ($0 \le \phi \le 1$) linked to a partitioning of Darcy-Weisbach friction coefficient f into a form-drag term, f_d, and a bed-friction term, f_s,

$$f = f_d + f_s, \tag{5}$$

leading to Moog and Jirka (1999b)

$$\phi = 1 - f_s/f. \tag{6}$$

$\phi = 0$ corresponds to pure bed friction, while $\phi = 1$ corresponds to pure form drag.

2.2. Empirical Gas Transfer Velocity Models

The most widely used empirical scaling for k_{600} was proposed by Raymond et al. (2012), as a set of seven alternative expressions for k_{600} as a function of different combinations of velocity, slope, depth, discharge, and/or Froude number, calibrated on 559 distinct measurements on US rivers. All seven expressions (denoted as Model R12, n. 1 to n. 7—see Table S1 in Supporting Information S1 for the complete list of equations) have an explicit dependence on the slope and velocity product $SV \propto \varepsilon_d$ in the form of $k_{600} \propto (SV)^\alpha$, with $\alpha \in (0.76 - 1)$. R12 n. 4 and 5, in particular, have the weakest and strongest sensitivity to SV across the whole set, and can be written as a function of ε_d as follows:

$$\text{Model R12 n. 4:} \qquad k_{600}(\varepsilon_d) = k_d = 167.8\,\varepsilon_d^{0.76} \quad (\text{m/d}) \tag{7}$$

$$\text{Model R12 n. 5:} \qquad k_{600}(\varepsilon_d) = k_d = 2.02 + 289.6\,\varepsilon_d \quad (\text{m/d}) \tag{8}$$

where we used k_d to denote k_{600} when calculated as a function of ε_d alone. The water depth appears in only four of the R12 models (n. 1, 2, 6, and 7—see Table S1 in Supporting Information S1), either explicitly or through the Froude number or discharge, and affects k_{600} relatively weakly as $k_{600} \propto H^{\beta}$, with $\beta \in (0.01 - 0.58)$.

More recently, Ulseth et al. (2019) introduced a new semi-empirical model for k_{600}, also calculated as a function of ε_d only:

$$\text{Model U19:}\ k_{600}(\varepsilon_d) = k_d = \begin{cases} 22.2\,\varepsilon_d^{0.35} \quad (\text{m/d}), & \text{when } \varepsilon_d \le 0.02\text{m}^2/\text{s}^3 \\ 620.2\,\varepsilon_d^{1.18} \quad (\text{m/d}), & \text{when } \varepsilon_d > 0.02\text{m}^2/\text{s}^3 \end{cases} \tag{9}$$

This model was derived with a specific focus on steep and high-energy mountain streams ($\varepsilon_d > 0.02$ m^2/s^3), where the sensitivity of k_{600} to variations in ε_d increases due to surface breaking and the consequent activation of bubble-mediated transfer (Ulseth et al., 2019).

Model U19 (Equation 9) suggests the scaling of k_{600} with ε_d rather than ε_s, consistently with its focus on high-energy streams. Of the seven R12 models, only those including a depth term (n. 1, 2, 6, and 7) can account for the different scaling of k_{600} at large submergence. These models fitted the calibration data better, but they also predicted an increase in k_{600} at stream orders larger than 4, which was deemed unphysical (Raymond et al., 2012). As a result, all the most recent estimates of global riverine gas emissions have been obtained through models that are not consistent with theoretical expectations in high-submergence conditions, specifically through model R12 n. 5 (e.g., Lauerwald et al., 2015; Raymond et al., 2013), or through the combination of R12 n.5 and U19 for large slope streams (e.g., Liu et al., 2022).

2.3. Model Calibration Data Sets

The U19 model (Equation 9) and R12 model (Equations 7 and 8) were calibrated on two largely overlapping data sets. Here, we focused on the larger U19 calibration data set (hereafter the U19 data set), which consisted of 718 independent measurements of k_{600}, discharge Q, slope S, velocity V, channel width W, and estimated depth H. The calibration of the R12 models was based on 559 of these measurements. Part of these data had a mistake in the conversion of discharge and/or width data from imperial to SI units, which has been corrected. The analysis by Ulseth et al. (2019) was not affected since it only employed the velocity data. All k_{600} data in the U19 (and R12) data set were measured using a gas tracing approach. Presently, this is regarded as the most accurate approach since it avoids the limitations of measurement chambers, such as the artificial enhancement of turbulence and the difficult deployment in high-energy and/or wavy flows (Hall & Ulseth, 2020). However, the method only applies to relatively small rivers. The whole U19 data set had a median depth of 0.22 m (5th to 95th percentile: 0.06–0.92 m) and a median discharge of 0.25 m^3/s (0.005–9.32 m^3/s).

3. Methodology

3.1. Estimation of the Relative Submergence

Different drivers of shear stress and turbulence distributions in low- and high-submergence conditions result in a different scaling of the hydraulic flow resistance. For instance, the Darcy-Weisbach friction factor, $f = 8u_*^2/V^2$, can be expressed as the sum of two power functions of H/D, as follows (Ferguson, 2007),

$$\frac{f}{8} = \left(\frac{u_*}{V}\right)^2 = \frac{1}{c_1^2}\left(\frac{H}{D}\right)^{-1/3} + \frac{1}{c_2^2}\left(\frac{H}{D}\right)^{-2}, \tag{10}$$

where $c_1 = 7.5$ and $c_2 = 2.36$ (Ferguson, 2007) are empirical weighting parameters. In the large-submergence limit, Equation 10 has a $f_s \propto (H/D)^{-1/3}$ dependence that derives from a Manning-type 1/6 power function velocity

profile, and is representative of bed-friction-dominated conditions. The small-submergence limit follows $f_d \propto (H/D)^{-2}$ and agrees with the linear velocity profile expected in form-drag-dominated conditions. The partitioning of f according to Equation 10, therefore, is consistent with Equation 5.

Equation 10 is equivalent to the following

$$\frac{gSH}{V^2} = \frac{1}{c_1^2}\left(\frac{H}{D}\right)^{-1/3} + \frac{1}{c_2^2}\left(\frac{H}{D}\right)^{-2}. \tag{11}$$

Equation 11 has been used to predict V up to very low values of H/D in step-pool streams with emergent clasts (Comiti et al., 2007; Lee & Ferguson, 2002). Its validity was recently confirmed also for high-submergence sand/gravel bed rivers, while it was found slightly underestimating the flow resistance in sand-bed rivers with bedforms (Ferguson & Recking, 2025). Here, we propose a novel application of Equation 10 as a means to estimating the unknown submergence H/D as a function of S, H, and V: By linking the friction factor partitioning in Equation 10 with Equation 5, we approximate $f_s \approx (8/c_1^2)(H/D)^{-1/3}$, which, by substitution into Equation 6, leads to

$$\phi = \left[1 + \left(\frac{c_2}{c_1}\right)^2 \left(\frac{H}{D}\right)^{5/3}\right]^{-1}. \tag{12}$$

H/D can be calculated by inverting Equation 11 numerically, and substituted into Equation 12 to determine ε_ϕ via Equation 4. Then, the submergence-corrected gas transfer velocity, $k_\phi = k_{600}(\varepsilon_\phi)$ can be estimated by replacing ε_d with ε_ϕ in Equations 7 and 8, or Equation 9. The ratio k_ϕ/k_d is a correction factor that enables accounting for the different gas transfer scaling at large submergence. For models R12 n.4 (Equation 7) and U19 (Equation 9), the correction factor takes the following form:

$$\frac{k_\phi}{k_d} = \left(\frac{\varepsilon_\phi}{\varepsilon_d}\right)^\alpha = \left[1 - (1-\phi)\left(1 - \frac{u_*}{V}\right)\right]^\alpha, \tag{13}$$

which can be demonstrated to be only a function of H/D through Equation 6 and Equation 11. Large lowland rivers have $u_*/V \ll 1$ and $\phi < 1$. Therefore, we expect their corrected gas transfer velocity, k_ϕ, to be potentially much smaller than the prediction based on the small-submergence scaling, k_d.

3.2. Validation of the Submergence Reconstruction

The determination of the friction factor as a function of relative submergence through Equation 11 (i.e., the forward problem) has been validated extensively (Ferguson & Recking, 2025; Lee & Ferguson, 2002). We tested the accuracy of submergence reconstruction as a function of bulk hydraulic parameters (i.e., the inverse problem) on a subset of 39 measurements (the only ones that included a record of bed roughness size) extracted from the U19 data set. The measurements belonged to eight Alpine streams and showed a significant correlation between median streambed roughness size, D_{50}, and k_{600} (Ulseth et al., 2019). The generally good agreement between measured and reconstructed submergence (Text S1 and Figure S1 in Supporting Information S1) confirms the suitability of the approach to reconstruct the submergence information when not known. Larger deviations between measurements and predictions were observed for two high-altitude sites (Valsorey, 1,937 and 2,161 m a.s.l., respectively) dominated by a step-pool morphology (see Ulseth et al., 2019, Figure S4). This could indicate a loss of validity of Equation 11 under non-homogeneous flow conditions, or could result from a different definition of bed roughness height. While step-pool conditions were predominant in the validation subset, which was focused on steep mountain streams, they are assumed to be less significant for the rest of the U19 data set and for global rivers.

3.3. Calculation of Global CO_2 Emissions From Rivers

We quantified the impact of the submergence correction on the estimates of global annual CO_2 riverine emissions by integrating global river geometry (Yamazaki et al., 2019) and hydrology databases (Lin et al., 2019) with a recent global dissolved CO_2 concentration model (Liu et al., 2022). Average river width, depth, and velocity were

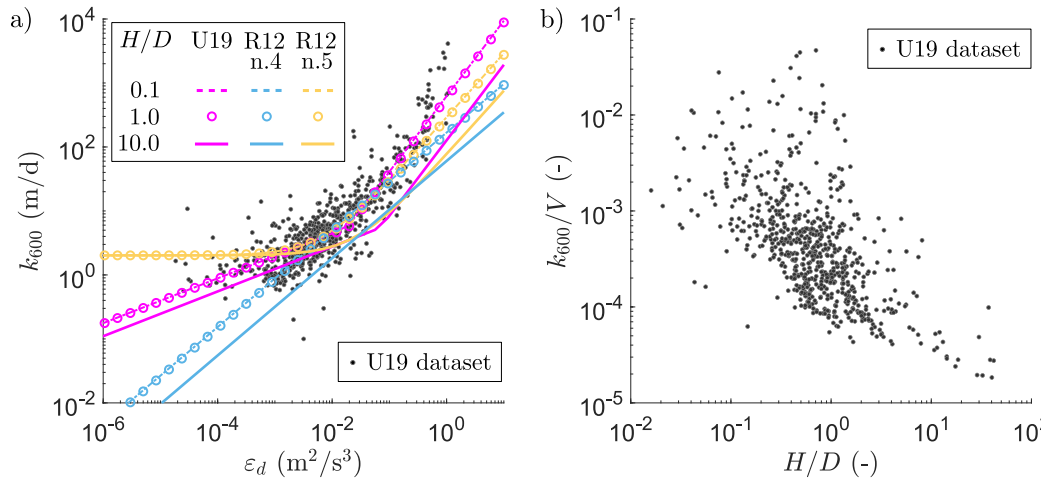

Figure 2. (a) Calibration data (black dots) for the empirical k_{600} models U19 (magenta—Equation 9), R12 n. 4 (blue—Equation 7), and R12 n. 5 (yellow—Equation 8) are limited to a narrow range in stream power ε_d. Outside of that range, the models deviate significantly. Accounting for the effects of relative submergence H/D would shift the models toward the right (larger ε_d). The shift is negligible between $H/D = 0.1$ (dashed) and $H/D = 1$ (circles), but increases between $H/D = 1$ and $H/D = 10$ (solid). (b) Reconstructing the relative submergence H/D for the U19 data set reveals a decrease in non-dimensionalized gas exchange velocity k_{600}/V toward larger H/D.

estimated as a function of the discharge Q through a set of empirical hydraulic geometry scaling equations (Raymond et al., 2012). More details about these calculations are provided in the Text S2 in Supporting Information S1. We estimated the relative submergence for every reach based on Equation 11, and calculated the gas transfer velocity using Equations 7 and 8, or Equation 9, with and without the high-submergence correction. Finally, we computed CO_2 emissions from each single reach as $ECO_2 = k_{600}A(C - C_{eq})(600/Sc)^{0.5}$, where A is the reach surface area. The emissions correction was quantified as $\left(ECO_2^{(\phi)} - ECO_2^{(d)}\right)/ECO_2^{(\phi)}$, where superscripts (d) and (ϕ) denote the values calculated using $k_{600} = k_d$ or $k_{600} = k_\phi$, respectively.

4. Results

4.1. Representation of Gas Exchange Drivers Within the U19 Data Set

The three empirical models of Equations 7 and 8, and Equation 9 predict similar values of k_{600} for ε_d between 10^{-3} and 10^{-1} m^2/s^3, which includes the majority of the U19 data set (Figure 2a). All models have an asymptotic $k_{600} \propto \varepsilon^\alpha$ behavior at low ($\varepsilon_d < 10^{-3}$ m^2/s^3) and high energy ($\varepsilon_d > 10^{-2}$ m^2/s^3), represented by the log-log gradient α. The increase in α at high energy for models U19 (Equation 9: $\alpha = 0.35$ to 1.18) and R12 n. 5 (Equation 8: $\alpha = 0$ to 1) represents the activation of bubble-mediated gas exchange (Ulseth et al., 2019). The theoretical surface renewal model (Lamont & Scott, 1970) ($\alpha = 0.25$) falls between the R12 n. 5 ($\alpha = 0$) and U19 ($\alpha = 0.35$) models at low ε_d. Model R12 n. 4 (Equation 7) has a constant $\alpha = 0.76$. The three empirical models deviate substantially (by up to one order of magnitude) at $\varepsilon_d < 10^{-4}$ m^2/s^3, where calibration data is scarce. Replacing ε_d with ε_ϕ to account for submergence effects corresponds to shifting the models toward larger ε_d, since $\varepsilon_\phi \leq \varepsilon_d$. The shift is non-linear in H/D, and increases with α. The shift is negligible for $H/D \leq 1$, confirming that ε_d is a good approximation of ε_ϕ at low submergence, then it increases rapidly with $H/D > 10$. According to the R12 n. 5 model (Equation 8), k_{600} tends asymptotically to ≈ 2.02 m/d when ε_d is small. Replacing ε_d with ε_ϕ in this case has no effect on k_{600}, which remains approximately constant and independent of the submergence in low-energy rivers. This asymptotic behavior is specific to the R12 n. 5 model, and is not supported by either theory or measurements, since values of k_{600} significantly lower than 2 m/d appear in the U19 data set and have been documented especially in large rivers (Alin et al., 2011; Striegl et al., 2012).

Plotting the U19 data as a function of the reconstructed submergence reveals a higher exchange-to-transport ratio, k_{600}/V, at low H/D (Figure 2b), confirming the expected enhancement of turbulent mixing by larger roughness. k_{600}/V is maximum for $H/D \sim 1$. The largest k_{600} data correspond to conditions where gas exchange was

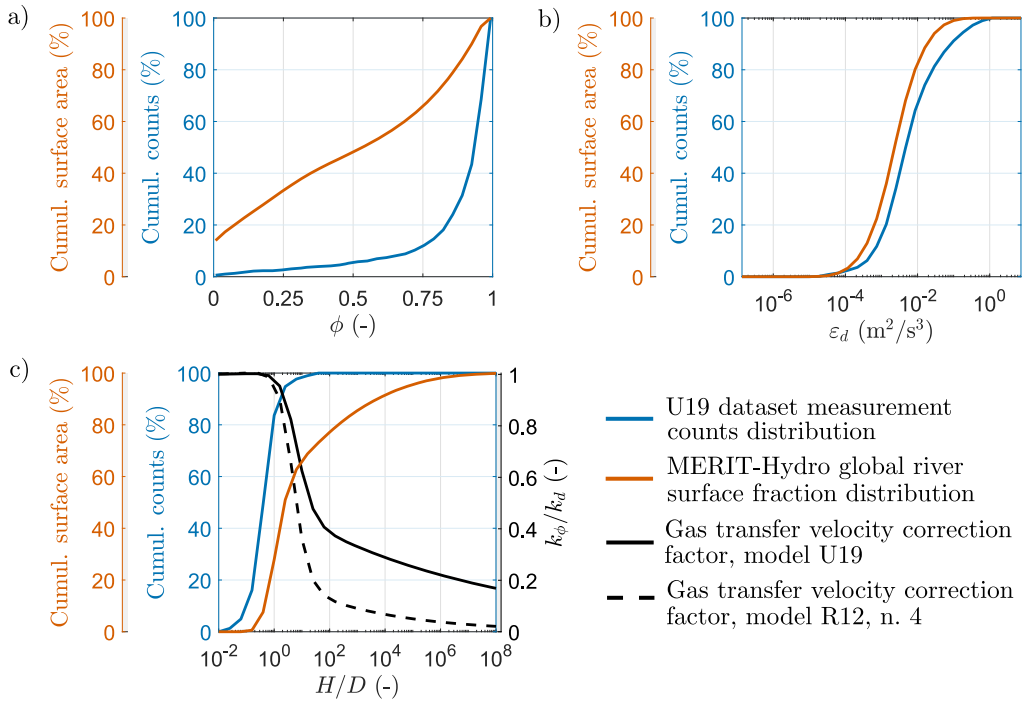

Figure 3. The U19 data set (blue) and global rivers (orange) have significantly different cumulative distributions of partitioning coefficient ϕ (a), total stream power ε_d (b), and relative submergence H/D (c). The factor k_ϕ/k_d represents the correction that should be applied to empirical models to account for the different drivers of turbulent mixing at large submergence. k_ϕ/k_d decreases rapidly to between 0.4 (model U19) and 0.13 (model R12, n.4) at $H/D \geq 100$. Existing empirical models cannot account for these effects because their calibration data (the U19 data set) includes mostly conditions where $k_\phi/k_d \approx 1$ (c). Note that the U19 distribution is expressed in terms of number of measurements (counts), while the MERIT-Hydro distribution represents the fraction of global river surface.

enhanced by surface breaking (Ulseth et al., 2019). The peak in k_{600}/V distribution could indicate that breaking is facilitated by the coupling of roughness and flow scales, although the large scatter in data suggests that submergence is not the only driver of surface breaking.

The reconstructed submergence data in Figure 2a fall predominantly within a relatively narrow interval between $H/D = 0.1$ and $H/D = 3$. These values are representative of relatively shallow rivers and streams. For comparison, we reconstructed the values of ϕ, ε_d, and H/D for almost 3 million river reaches by applying Equations 3, 11, and 12 to global river databases, and quantified their area-weighted distributions. Compared to the U19 data set, global rivers have lower ϕ (Figure 3a), lower ε_d (Figure 3b), and higher H/D (Figure 3c). In particular, rivers with $\phi \leq 0.8$ represent 70% of the global river surface but account for less than 15% of data in the U19 data set (Figure 3a). The gas transfer velocity correction factor k_ϕ/k_d (Equation 13) decreases rapidly between $H/D = 1$ and $H/D = 100$ for both models U19 and R12 n. 4 (model R12 n. 5 is not shown in Figure 3c since k_ϕ/k_d cannot be expressed only as a function of H/D, but it also depends on ε_d). At large submergence ($H/D > 100$), k_ϕ/k_d is lower than 0.4 (model U19) or 0.13 (model R12, n.4), meaning that accounting for the lower turbulence dissipation rate at large submergence would yield a 60% (model U19) to 87% (model R12, n. 4) reduction in gas transfer velocity relative to estimations based on ε_d. The condition $H/D > 100$ represents 23% of the total river surface, but is completely absent in the U19 data set, which explains why submergence and depth have not been identified as drivers of gas transfer velocity in the empirical models calibrated on those data.

4.2. Impact of the Data Set Bias on Riverine Greenhouse Gas Emission Estimates

Our estimates of global CO_2 emission from rivers vary considerably depending on the gas transfer velocity model and on whether the high-submergence correction is applied or not (Table S2 in Supporting Information S1). The standard (without correction) R12 n. 5 model (Equation 8) predicts 2.23 (1.85–2.61) Pg CO_2 y^{-1} of global riverine emissions. Previous estimates based on the same R12 n. 5 model ranged between a very similar value of 2.38

10.1029/2026GL121645

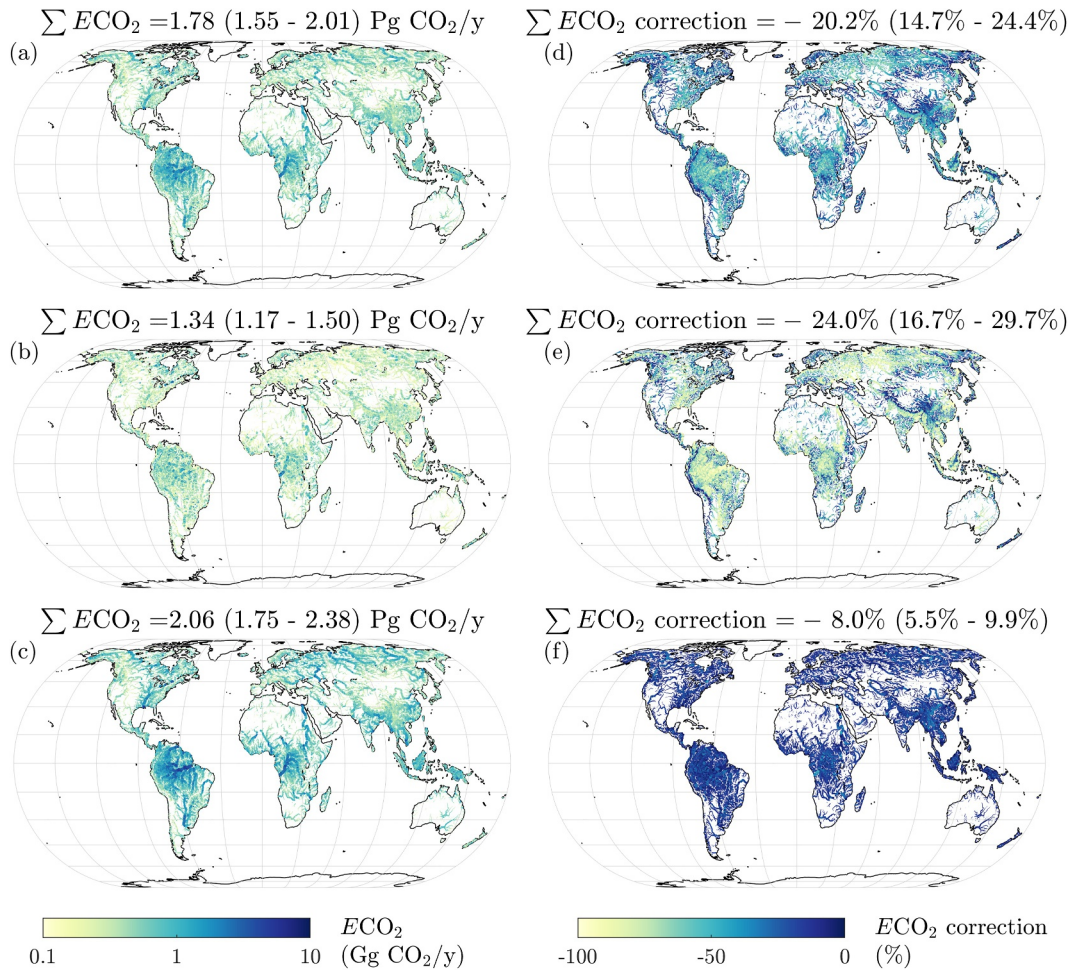

Figure 4. Accounting for the different scaling of gas exchange velocity at large-submergence, global CO_2 emissions ($\sum ECO_2$) are predicted to be significantly smaller and more uncertain than previously considered. The submergence-corrected distributions of riverine CO_2 emissions (a–c) reveal a weaker contribution of large rivers, but the distribution of the correction factor (d–f) varies significantly between the three considered gas transfer velocity models: U19 (a, d); R12 n. 4 (b, e); R12 n. 5 (c–f).

(1.77–3.10) Pg CO_2 y^{-1} (Lauerwald et al., 2015) to a much larger estimate of 7.33 (6.60–8.07) Pg CO_2 y^{-1} (Liu et al., 2022) (Table S3 in Supporting Information S1). The latter includes emissions from headwater streams that are not included in the MERIT-Hydro database and are missed by our calculations. Repeating the calculations using the same R12 n. 5 model but including the high-submergence correction, we estimated an 8% decrease in emissions: 2.06 (1.75–2.38) Pg CO_2 y^{-1}. In this case, the correction was limited to a few high-submergence and intermediate-slope rivers (Figures 4c and 4f), since the R12 n. 5 model predicts a constant gas transfer rate of 2 m/d for low-slope lowland rivers (Figure 2a).

The U19 (Equation 9) and R12 n. 4 (Equation 7) models are much more sensitive to large-submergence corrections. Applying the correction to these models resulted in a 20% (U19) to 24% (R12 n. 4) decrease in global CO_2 emissions. This reflects a very strong reduction (up to 47%, see Table S2 in Supporting Information S1) in emissions from large, lowland, and high-submergence rivers (Figures 4d and 4e), where the impact on emissions was amplified by the large surface area and generally larger dissolved CO_2 concentrations (Liu et al., 2022). The corrected emissions estimated with the U19 and R12 n. 4 models were 1.34 (1.17–1.50) Pg CO_2 y^{-1} and 1.78 (1.55–2.01) Pg CO_2 y^{-1}, respectively (Figures 4b and 4c).

5. Discussion

The predominance of low-submergence conditions in the U19 data set (including the data used by Raymond et al. (2012)) is not surprising given their focus on small rivers and streams, and considering the range of applicability of gas tracing measurements. This explains why empirical models calibrated on those data scale with the low-submergence and drag-dominated turbulence dissipation term ε_d rather than with the high-submergence and friction-dominated term ε_s. However, these models are also commonly applied to lowland rivers (e.g., Lauerwald et al., 2015; Liu et al., 2022; Raymond et al., 2013), where (a) the drivers of near-surface turbulent mixing and therefore the scaling of the gas transfer velocity with bulk flow parameters are different; and (b) k_{600} predictions by different models differ widely, and the lack of data prevents the identification of a single most accurate model. Considering both the correction for the different scaling of turbulence dissipation at large submergence, and the variability associated with the choice of one of the three gas transfer velocity models, we suggest revising global CO_2 estimates from 2.23 (1.85–2.61) Pg CO_2 y^{-1} (calculated with the standard R12 n. 5 model without large-submergence correction) to between 1.17 Pg CO_2 y^{-1} and 2.38 Pg CO_2 y^{-1} (lower and upper limits of the submergence-corrected R12 n. 4 and n. 5 models, respectively). This change corresponds to a reduction of between 9% and 37% in global emissions, and a doubling of the relative uncertainty (size of confidence intervals relative to the magnitude of the emissions), from 34% to 68%. Both effects are ultimately a consequence of the lack of high-submergence data in the empirical models calibration data set.

Our analysis assumes the validity of the gas transfer velocity partitioning and scalings proposed by Moog and Jirka (1999a), Moog and Jirka (1999b). While the validity of the low-submergence scaling (Equation 3) is well supported by the existing semi-empirical model (Ulseth et al., 2019), validating the existing high-submergence model (Moog & Jirka, 1999a) and/or extending the validity of empirical models to large-submergence rivers requires additional data at large submergence. Direct measurements of gas transfer velocity in lowland rivers have been reported by various authors (e.g., Alin et al., 2011; Beaulieu et al., 2012; Sawakuchi et al., 2017), but their integration in the calibration data sets for empirical models remains difficult, since measuring reach-averaged slope, depth, velocity, and relative submergence is very challenging, and gas transfer velocity measurements at large flows rely on floating chambers, which can strongly overestimate the gas transfer velocity (Vachon et al., 2010). Other processes, such as the presence of bedforms (Bennett & Best, 1995) or wind (Alin et al., 2011; Beaulieu et al., 2012), can enhance turbulent mixing and increase the effective gas transfer velocity, especially in large rivers (Wang et al., 2021). In that case, the large-submergence correction proposed here may lead to underestimating the true magnitude of exchange fluxes locally, and Ferguson's (2007) partitioning equation may lose validity. Local predictions of the gas transfer velocity based on empirical models remain subject to very large uncertainties despite the large-submergence correction, and direct measurements should be conducted whenever possible (Hall & Ulseth, 2020).

6. Conclusions

The most widely used empirical and semi-empirical models for the gas transfer velocity in rivers (Raymond et al., 2012; Ulseth et al., 2019) have been calibrated based on data from small rivers and streams with a low relative submergence. As such, they do not account for the expected change in the physical drivers of turbulent mixing between low- and high-submergence conditions. Unlike other random sources of uncertainty that may vanish with upscaling, the systematic bias introduced by submergence effects impacts gas exchange flux calculations at all scales. However, low-submergence models are commonly used to calculate gas fluxes in rivers with a wide range of submergences extending beyond the range used for their calibration, for example, to compute global riverine greenhouse gas emission estimates (Lauerwald et al., 2015; Liu et al., 2022) that inform regional and global carbon budgets (Lauerwald et al., 2024), such as the IPCC report (Canadell et al., 2021).

Here, we presented a straightforward and physically consistent approach to correct gas exchange calculations for the different drivers of gas transfer velocity at large submergence, even when bed roughness and submergence data are not available (i.e., in the large majority of cases). Taking into account this correction, we determined that the contribution of large lowland (high-submergence) rivers to greenhouse gas emissions may have been significantly overestimated in past calculations. We estimate that global riverine CO_2 emissions should be revised downward by between 9% and 37%, and that their uncertainties should be increased to 68% to account for large discrepancies between empirical gas transfer velocity models, caused by a lack of experimental data at large submergence.

Ultimately, our analysis calls into question the validity of present widespread operational gas transfer velocity models in high-submergence rivers. Testing and refining these models requires significant efforts across multiple areas of research to improve the understanding and characterization of gas exchange and its drivers, and to build representative and more complete data sets, especially in high-submergence rivers. This requires (a) overcoming current limitations in measuring gas exchange and its drivers at a large scale (promising steps in this direction have been made with inverse modeling applied to CO_2 and/or O_2 data, e.g., Diamond & Bertuzzo, 2025, Dolcetti et al., 2025), and (b) making the systematic measurement of key parameters, such as the relative submergence, an integral part of new valuable plans for monitoring and observation of rivers biogeochemistry (e.g., Dean & Battin, 2024). By providing the means to account for different physical drivers of gas exchange as a function of submergence, this work offers a rigorous yet practical basis for more accurate and robust models that better capture the complexity of gas exchange across global river systems.

Conflict of Interest

The authors declare no conflicts of interest relevant to this study.

Availability Statement

Data and Matlab scripts related to this work, including estimated submergence, gas transfer velocities, and CO_2 emissions for the MERIT-Hydro river reaches are openly available at the following URL: https://doi.org/10.5281/zenodo.15675363 (Dolcetti, 2025).

Acknowledgments
Financed by the European Union—Next Generation EU, Mission 4 Component 2—CUP 20222W5WXC. The Authors are grateful to A. J. Ulseth and R. Hall for kindly providing additional information and clarification about their data set. Open access publishing facilitated by Universita degli Studi di Trento, as part of the Wiley - CRUI-CARE agreement.

References

Alin, S. R., de Fátima FL Rasera, M., Salimon, C. I., Richey, J. E., Holtgrieve, G. W., Krusche, A. V., & Snidvongs, A. (2011). Physical controls on carbon dioxide transfer velocity and flux in low-gradient river systems and implications for regional carbon budgets. *Journal of Geophysical Research*, *116*(G1), G01009. https://doi.org/10.1029/2010jg001398

Battin, T. J., Lauerwald, R., Bernhardt, E. S., Bertuzzo, E., Gener, L. G., Hall, R. O., Jr., et al. (2023). River ecosystem metabolism and carbon biogeochemistry in a changing world. *Nature*, *613*(7944), 449–459. https://doi.org/10.1038/s41586-022-05500-8

Beaulieu, J. J., Shuster, W. D., & Rebholz, J. A. (2012). Controls on gas transfer velocities in a large river. *Journal of Geophysical Research*, *117*(G2). https://doi.org/10.1029/2011jg001794

Bennett, S., & Best, J. (1995). Mean flow and turbulence structure over fixed, two-dimensional dunes: Implications for sediment transport and bedform stability. *Sedimentology*, *42*(3), 491–513. https://doi.org/10.1111/j.1365-3091.1995.tb00386.x

Canadell, J. G., Monteiro, P. M. S., Costa, M. H., Cotrim da Cunha, L., Cox, P. M., Eliseev, A. V., et al. (Eds.), Climate change 2021: The physical science basis. Contribution of working group I to the sixth assessment report of the intergovernmental panel on climate change (pp. 673–816). Cambridge University Press. https://doi.org/10.1017/9781009157896.007

Comiti, F., Mao, L., Wilcox, A., Wohl, E. E., & Lenzi, M. A. (2007). Field-derived relationships for flow velocity and resistance in high-gradient streams. *Journal of Hydrology*, *340*(1–2), 48–62. https://doi.org/10.1016/j.jhydrol.2007.03.021

Danckwerts, P. V. (1951). Significance of liquid-film coefficients in gas absorption. *Industrial & Engineering Chemistry*, *43*(6), 1460–1467. https://doi.org/10.1021/ie50498a055

Dean, J. F., & Battin, T. J. (2024). Future directions for river carbon biogeochemistry observations. *Nature Water*, *2*(3), 219–222. https://doi.org/10.1038/s44221-024-00207-8

Diamond, J. S., & Bertuzzo, E. (2025). A coupled O_2-CO_2 model for joint estimation of stream metabolism, O-C stoichiometry, and inorganic carbon fluxes. *Journal of Geophysical Research: Biogeosciences*, *130*(4), e2024JG008401. https://doi.org/10.1029/2024jg008401

Dolcetti, G. (2025). On the biases of empirical riverine gas transfer velocity models at high submergence—Supplementary data and software [Dataset]. https://doi.org/10.5281/zenodo.15675363

Dolcetti, G., Piccolroaz, S., Bruno, M. C., Calamita, E., Larsen, S., Zolezzi, G., & Siviglia, A. (2025). Quantification of carbopeaking and CO_2 fluxes in a regulated Alpine river. *Water Resources Research*, *61*(2), e2024WR037834. https://doi.org/10.1029/2024wr037834

Ferguson, R. (2007). Flow resistance equations for gravel-and boulder-bed streams. *Water Resources Research*, *43*(5). https://doi.org/10.1029/2006wr005422

Ferguson, R., & Recking, A. (2025). Flow resistance and hydraulic geometry in gravel- and boulder-bed rivers. *Water Resources Research*, *61*(3), e2024WR038852. https://doi.org/10.1029/2024wr038852

Hall, R. O. J., & Ulseth, A. J. (2020). Gas exchange in streams and rivers. *Wiley Interdisciplinary Reviews: Water*, *7*(1), e1391. https://doi.org/10.1002/wat2.1391

Katul, G., & Liu, H. (2017). Multiple mechanisms generate a universal scaling with dissipation for the air-water gas transfer velocity. *Geophysical Research Letters*, *44*(4), 1892–1898. https://doi.org/10.1002/2016gl072256

Lamont, J. C., & Scott, D. S. (1970). An eddy cell model of mass transfer into the surface of a turbulent liquid. *AIChE Journal*, *16*(4), 513–519. https://doi.org/10.1002/aic.690160403

Lauerwald, R., Allen, G. H., Deemer, B. R., Liu, S., Maavara, T., Raymond, P., et al. (2023). Inland water greenhouse gas budgets for RECCAP2: 2. Regionalization and homogenization of estimates. *Global Biogeochemical Cycles*, *37*(5), e2022GB007658. https://doi.org/10.1029/2022gb007658

Lauerwald, R., Bastos, A., McGrath, M. J., Petrescu, A. M. R., Ritter, F., Andrew, R. M., et al. (2024). Carbon and greenhouse gas budgets of Europe: Trends, interannual and spatial variability, and their drivers. *Global Biogeochemical Cycles*, *38*(8), e2024GB008141. https://doi.org/10.1029/2024gb008141

Lauerwald, R., Laruelle, G. G., Hartmann, J., Ciais, P., & Regnier, P. A. G. (2015). Spatial patterns in CO_2 evasion from the global river network. *Global Biogeochemical Cycles*, *29*(5), 534–554. https://doi.org/10.1002/2014gb004941

Lee, A. J., & Ferguson, R. I. (2002). Velocity and flow resistance in step-pool streams. *Geomorphology*, *46*(1–2), 59–71. https://doi.org/10.1016/s0169-555x(02)00054-5

Lin, P., Pan, M., Beck, H. E., Yang, Y., Yamazaki, D., Frasson, R., et al. (2019). Global reconstruction of naturalized river flows at 2.94 million reaches. *Water Resources Research*, *55*(8), 6499–6516. https://doi.org/10.1029/2019wr025287

Liu, S., Kuhn, C., Amatulli, G., Aho, K., Butman, D. E., Allen, G. H., et al. (2022). The importance of hydrology in routing terrestrial carbon to the atmosphere via global streams and rivers. *Proceedings of the National Academy of Sciences*, *119*(11), e2106322119. https://doi.org/10.1073/pnas.2106322119

Lorke, A., & Peeters, F. (2006). Toward a unified scaling relation for interfacial fluxes. *Journal of Physical Oceanography*, *36*(5), 955–961. https://doi.org/10.1175/jpo2903.1

Moog, D. B., & Jirka, G. H. (1999a). Air-water gas transfer in uniform channel flow. *Journal of Hydraulic Engineering*, *125*(1), 3–10. https://doi.org/10.1061/(asce)0733-9429(1999)125:1(3)

Moog, D. B., & Jirka, G. H. (1999b). Stream reaeration in nonuniform flow: Macroroughness enhancement. *Journal of Hydraulic Engineering*, *125*(1), 11–16. https://doi.org/10.1061/(asce)0733-9429(1999)125:1(11)

Nezu, I., & Nakagawa, H. (1993). *Turbulence in open-channel flows*. A.A. Balkema.

Raymond, P. A., Hartmann, J., Lauerwald, R., Sobek, S., McDonald, C., Hoover, M., et al. (2013). Global carbon dioxide emissions from inland waters. *Nature*, *503*(7476), 355–359. https://doi.org/10.1038/nature12760

Raymond, P. A., Zappa, C. J., Butman, D., Bott, T. L., Potter, J., Mulholland, P., et al. (2012). Scaling the gas transfer velocity and hydraulic geometry in streams and small rivers. *Limnology and Oceanography: Fluids and Environments*, *2*(1), 41–53. https://doi.org/10.1215/21573689-1597669

Sawakuchi, H. O., Neu, V., Ward, N. D., Barros, M. D. L. C., Valerio, A. M., Gagne-Maynard, W., et al. (2017). Carbon dioxide emissions along the lower Amazon River. *Frontiers in Marine Science*, *4*, 76. https://doi.org/10.3389/fmars.2017.00076

Striegl, R. G., Dornblaser, M. M., McDonald, C. P., Rover, J., & Stets, E. G. (2012). Carbon dioxide and methane emissions from the Yukon River system. *Global Biogeochemical Cycles*, *26*(4). https://doi.org/10.1029/2012gb004306

Ulseth, A. J., Hall, R. O., Jr., Boix Canadell, M., Madinger, H. L., Niayifar, A., & Battin, T. J. (2019). Distinct air–water gas exchange regimes in low-and high-energy streams. *Nature Geoscience*, *12*(4), 259–263. https://doi.org/10.1038/s41561-019-0324-8

Vachon, D., Prairie, Y. T., & Cole, J. J. (2010). The relationship between near-surface turbulence and gas transfer velocity in freshwater systems and its implications for floating chamber measurements of gas exchange. *Limnology and Oceanography*, *55*(4), 1723–1732. https://doi.org/10.4319/lo.2010.55.4.1723

Wang, J., Bombardelli, F. A., & Dong, X. (2021). Physically based scaling models to predict gas transfer velocity in streams and rivers. *Water Resources Research*, *57*(3), e2020WR028757. https://doi.org/10.1029/2020wr028757

Yamazaki, D., Ikeshima, D., Sosa, J., Bates, P. D., Allen, G. H., & Pavelsky, T. M. (2019). MERIT Hydro: A high-resolution global hydrography map based on latest topography dataset. *Water Resources Research*, *55*(6), 5053–5073. https://doi.org/10.1029/2019wr024873

References From the Supporting Information

Altenau, E. H., Pavelsky, T. M., Durand, M. T., Yang, X., Frasson, R. P. D. M., & Bendezu, L. (2021). The Surface Water and Ocean Topography (SWOT) Mission River Database (SWORD): A global river network for satellite data products. *Water Resources Research*, *57*(7), e2021WR030054. https://doi.org/10.1029/2021wr030054

Fick, S. E., & Hijmans, R. J. (2017). WorldClim 2: New 1-km spatial resolution climate surfaces for global land areas. *International Journal of Climatology*, *37*(12), 4302–4315. https://doi.org/10.1002/joc.5086

Liu, S. (2021). Monthly pCO_2, gas transfer velocity and CO_2 efflux rate in global streams and rivers (the GRADES River Networks) [Dataset]. *Dryad*. https://doi.org/10.5061/dryad.d7wm37pz9

Schneider, J. M., Rickenmann, D., Turowski, J. M., & Kirchner, J. W. (2015). Self-adjustment of stream bed roughness and flow velocity in a steep mountain channel. *Water Resources Research*, *51*(10), 7838–7859. https://doi.org/10.1002/2015wr016934

Wanninkhof, R. (1992). Relationship between wind speed and gas exchange over the ocean. *Journal of Geophysical Research*, *97*(C5), 7373–7382. https://doi.org/10.1029/92jc00188